Mechanism of Heterogeneous Reaction of Carbonyl Sulfide on Magnesium Oxide

Yongchun Liu, Hong He,* Wenqing Xu, and Yunbo Yu

State Key Laboratory of Environmental Chemistry and Ecotoxicology, Research Center for Eco-Environmental Science, Chinese Academy of Sciences, Beijing 100085, China

Received: December 29, 2006; In Final Form: March 13, 2007

Heterogeneous reaction of carbonyl sulfide (OCS) on magnesium oxide (MgO) under ambient conditions was investigated by in situ diffuse reflectance infrared Fourier transform spectroscopy (DRIFTS), quadrupole mass spectrometer (QMS), and density functional theory (DFT) calculations. It reveals that OCS can be catalytically hydrolyzed by surface hydroxyl on MgO to produce carbon dioxide (CO_2) and hydrogen sulfide (H_2S), and then H_2S can be further catalytically oxidized by surface oxygen or gaseous oxygen on MgO to form sulfite (SO_3^{2-}) and sulfate (SO_4^{2-}). Hydrogen thiocarbonate ($HSCO_2^-$) was found to be the crucial intermediate. Surface hydrogen sulfide (HS), sulfur dioxide (SO_2), and surface sulfite (SO_3^{2-}) were also found to be intermediates for the formation of sulfate. Furthermore, the surface hydroxyl contributes not only to the formation of $HSCO_2^-$ but also to $HSCO_2^-$ decomposition. On the basis of experimental results, the heterogeneous reaction mechanism of OCS on MgO was discussed.

1. Introduction

Carbonyl sulfide (OCS) is the most abundant sulfur compound in the atmosphere, with a rather uniform mixing ratio of about 500 pptv (parts per trillion by volume) in the troposphere.[1−3] Its tropospheric lifetime is greater than 1 year[1,2] and the global atmospheric lifetime is from 2 to 8.9 years calculated by different researchers.[2,4] Chin and Davis[2] have reported that about 0.64 $Tg\cdot yr^{-1}$ of OCS is transported to stratosphere from troposphere, where its photolysis is the important source of stratospheric sulfate layer[5] and sustains the Junge layer. Therefore, it is of interest to investigate the sources and sinks of OCS.

By now, numerous sinks have been identified, such as oxic soils, vegetation, homogeneous reaction with OH and O, and photolysis.[1−6] In recent years, there has been a great deal of interest in the heterogeneous chemistry of trace atmospheric gases on atmospheric particulates in the troposphere.[7−9] It is estimated that 3000−5000 Tg of particulate matter, in the form of soil dust, sea salt, organics, sulfate aerosol, and soot, and 1000−3000 Tg of mineral aerosols are emitted annually into the atmosphere.[10] On the other hand, atmospheric particulates have a large specific surface area, usually greater than 1 $m^2\cdot g^{-1}$.[11,12] Therefore, abundant and diverse atmospheric particulates can facilitate heterogeneous chemistry in the troposphere. More recently, a few studies have reported the heterogeneous reaction of OCS on atmospheric particles, Al_2O_3, SiO_2, Fe_2O_3, CaO, and MnO_2 at room temperature.[13−16] MgO is also a typical component of atmospheric particulates, whose content is about 6.1 wt % of the inorganic components in the Beijing area.[13,17] However, the reaction of OCS on MgO has not been reported yet. Therefore, it is significant to investigate the heterogeneous reaction of OCS on MgO to further understand the heterogeneous reaction of OCS on atmospheric particles.

In this paper, diffuse reflectance infrared Fourier transform spectroscopy (DRIFTS), quadrupole mass spectroscopy (QMS), and density functional theory (DFT) calculations were used to study the reaction mechanism of OCS on MgO. We found that MgO can catalyze the heterogeneous reaction of OCS under ambient conditions. Based on the information of intermediates and final products, a reaction mechanism was proposed.

2. Experimental Section

2.1. Materials. The MgO sample (A.R.) used in this experiment was supplied by Haizhong Chemical Plant in Tianjin. The impurities in MgO sample include Cl (0.01%), SO_4^{2-} (0.02%), PO_4^{3-} (0.003%), CO_3^{2-} (1.5%), Na (0.05%), K (0.005%), Ca (0.02%), Fe (0.005%), Cu (0.001%), Zn (0.005%), As (0.0001%), and Ba and Sr (0.005%). Before the DRIFTS measurement, the sample was pretreated in an in situ infrared chamber at 573 K in 100 $mL\cdot min^{-1}$ N_2 stream for 2 h.

All chemicals were used without further purification as follows: carbonyl sulfide (OCS, 2%, OCS/N_2, Scott Specialty Gases Inc.), N_2 and O_2 (99.99% purity, Beijing AP BEIFEN Gases Inc.), and P_2O_5 (A. R., The Sixth Chemical Plant in Tianjin).

2.2. Characterization of Sample. Nitrogen Brunauer−Emmett−Teller (BET) physisorption measurement was performed by use of Micromeritics ASAP 2000 automatic equipment. It was shown that the MgO sample has a total surface area of 14.6 $m^2\cdot g^{-1}$. The X-ray powder diffraction pattern was collected from 10° to 90° 2θ on a D/max-RB automatic powder X-ray diffractometer using Cu Kα irradiation. The sample was identified to be periclase with the three main 2θ peaks at 42.918°, 62.300°, and 78.622°. The diameter distribution was measured with a laser particle size analyzer, Masterizer 2000. The diameter was from 400 to 2500 μm with an average diameter of 759 μm.

2.3 Experimental Methods. In situ DRIFTS spectra were recorded on a NEXUS 670 (Thermo Nicolet Instrument Corp.) Fourier transform infrared (FT-IR) spectrometer, equipped with an in situ diffuse reflection chamber and a high-sensitivity mercury−cadmium−telluride (MCT) detector cooled by liquid N_2. The reference spectrum was measured after the pretreated

* Corresponding author: phone +86-10-62849123; fax +86-10-62923563; e-mail honghe@rcees.ac.cn.

10.1021/jp069015v CCC: $37.00
Published on Web 04/25/2007

sample was cooled to 303 K in nitrogen stream or simulated air. The infrared spectra were collected and analyzed by a computer with OMNIC 6.0 software. All spectra reported here were recorded at a resolution of 4 cm^{-1} for 100 scans.

The MgO sample (about 10 mg) for the in situ DRIFTS studies was finely ground and placed into a ceramic crucible in the in situ chamber. The total flow rate was 100 $mL \cdot min^{-1}$ in all of the flow systems, and the volume of reactor chamber in the closed system was 30 mL. N_2 (79%) and O_2 (21%) were mixed to simulate the composition of air. In all experiments, 2.0% OCS/N_2 was diluted to 1000 ppmv with high-purity N_2 or simulated air. Unless declared specially, the feed gas was not dried and is marked as moist OCS/air or moist OCS/N_2. The content of water in the feed gas was measured with a hygrometer, but it is lower than the lower limit of the hygrometer. In order to investigate the influence of water and surface hydroxyl on the reaction, reactant gases were dried with P_2O_5 and are marked as dry OCS/air or dry OCS/N_2. Gaseous products were determined on-line with a Hiden HPR20 QMS in flow system.

DFT calculations were performed to identify the intermediates. The Gaussian 98 program[18] was performed to optimize the structures and calculate the vibrational frequency for the calculated models (shown in Figure 4A), and the 3-21G basis set was employed to carry out the DFT-B3LYP calculations. The vibrational frequencies and intensities for the optimized models by the Gaussian 98 program were analyzed by the Gaussview 2.1 program package.

3. Results and Discussion

3.1. Heterogeneous Reaction of OCS on MgO in Closed System. Figure 1shows the dynamic changes of in situ DRIFTS spectra for the MgO sample at 303 K in closed system after moist OCS/air was added into the in situ infrared chamber for 3 min. The strong peaks of gaseous OCS appeared at 2071 and 2052 cm^{-1}.[14,15,19] A pair of peaks of gaseous CO_2 was observed at 2361 and 2341 cm^{-1}. The bands at 2578 cm^{-1} is the characteristic frequency of ν_s(SH) of surface HS.[20,21] The peak at 3755 cm^{-1} for surface hydroxyl[22] decreased in intensity as a function of time. The bands at 1659 and 1409 cm^{-1} were assigned to ν_{as}(OCO) and ν_s(OCO) of surface HCO_3^- species, which were accompanied by ν(OH) and δ(OH) at 3618 and 1225 cm^{-1}, respectively.[23−26] It should be noted that the frequency of $\delta(H_2O)$ is also close to 1659 cm^{-1}, which was accompanied by the broad band in the range of 3300−3500 cm^{-1}. Therefore, a similar experiment in dry air was performed. As shown in Figure 2, the intensity for all surface species on MgO in dry air was lower than that in moist air. This means the reaction was observably affected by water, as will be discussed in detail in section 3.3. However, the peaks at 3618, 1659, 1409, and 1225 cm^{-1} were also present when trace water was removed. Compared with Figure 1, the intensity of peaks in the range 3300−3500 cm^{-1} in Figure 2 was very weak while the intensity of the peak at 1659 cm^{-1} was still strong, indicating that HCO_3^- was mainly contributing to the band at 1659 cm^{-1}. In addition, a new negative peak at 3701 cm^{-1} due to the loss of another type of surface OH was also present, which means there were at least two kinds of surface hydroxyl participating in the reaction. The surface OH at 3755 cm^{-1} was more active than that at 3701 cm^{-1}, which corresponds to the basicity sequence of surface OH; namely, the higher the wavenumber, the stronger the basicity for surface OH.[27] For both cases, the peak intensities of CO_2 at 2341 and 2361 cm^{-1} increase with time at first and then decrease after a certain time. However, this trend is more obvious in dry air. These phenomena can be attributed to the adsorption process of CO_2 and the different surface coverage of bicarbonate and carbonate in moist and dry air. In Figure 2, a new band at 1000 cm^{-1} belonging to an unknown surface species also appeared.

In order to better understand the surface species, the DRIFTS spectrum in the range of 1150−1750 cm^{-1} after reaction for 10 min in Figure 1 was fitted by Peakfit based on the second-derivative spectrum,[28] as shown in Figure 3 with a correlation coefficient of 0.9994. The bands at 1379 and 1138 cm^{-1} were assigned to ν_{as}(SO) and ν_3(SO) of surface SO_4^{2-} species, respectively,[29−31] and the weak band at 1334 cm^{-1} is the ν_{as}(SO) band of physical adsorbed SO_2.[32,33] The appearance of a band at 1584 cm^{-1} indicates the formation of carbonate on the surface of MgO sample.[34] The bands at 1651, 1408, and 1220 cm^{-1} in Figure 3 were assigned to surface HCO_3^-.[23−26] Peaks from 1084 to 945 cm^{-1} (shown in Figures 1 and 2) were due to the absorption of surface HSO_3^- and SO_3^{2-}.[24,35,36] The assignment for the peak at 1273 and 1545 cm^{-1} is unsure yet and is temporarily marked as *X*.

It can be clearly seen in Figures 1 and 2 that the intensity of peaks of gaseous OCS(g) and surface OH(s) decreased with time, accompanied by the increase of HCO_3^-(s), CO_2(g), HSO_3^-/SO_3^{2-}(s), and SO_4^{2-}(s). However, the peak intensity at 1273 cm^{-1} increased initially and then decreased with time. This suggests that 1273 cm^{-1} ought to be the band of an intermediate. Furthermore, the intensity of peaks of HCO_3^- in dry air is lower than that in moist air, while the relative intensity between the peak at 1273 and 1225 cm^{-1} become stronger in dry air than that in moist air. That means the heterogeneous reaction of OCS on MgO also took place even without water, but the decomposition rate for intermediate at 1273 cm^{-1} was restrained to a great extent, which leads to accumulation of the intermediate.

Hoggan et al.[37] have proposed hydrogen thiocarbonate ($HSCO_2^-$) as the intermediate for hydrolysis of OCS on alumina and have reported the vibrational frequency of $HSCO_2^-$ at 1572 ν_{as}(OCO) and 1327 cm^{-1} ν_s(OCO) on alumina. In our previous studies, we also observed $HSCO_2^-$ at 1575 cm^{-1} as the intermediate for heterogeneous reaction of OCS on Al_2O_3 using DRIFTS.[13−14] Because they have the same products, namely, CO_2 and H_2S, the reaction intermediate of OCS on MgO probably should be the same as that on Al_2O_3. If *X* was related to the intermediate, in other words, $HSCO_2^-$ on MgO, there was a large discrepancy between the reported frequency in literature[13,14,37] and our experimental results (Figure 3). Consequently, theoretical calculations were performed to identify the vibrational frequency for $HSCO_2^-$ on MgO.

3.2. Vibrational Frequency of Hydrogen Thiocarbonate by DFT Calculations. More than 10 kinds of calculated models of $HSCO_2^-$ on MgO, including monodentate, bidentate, and bridging hydrogen thiocarbonate, were designed for DFT calculations. The bridging hydrogen thiocarbonate model (shown in Figure 4A) is the best one to be in agreement with the experimental results (Figure 3) when calculated vibrational frequency and relative intensity were simultaneously considered. As can be seen in Figure 4B, the ν_{as}(OCO) vibrational frequency of thiocarbonate was calculated at 1564 cm^{-1} with 130 $km \cdot mol^{-1}$ intensity, which is very close to the experimental value of 1545 cm^{-1}, and the ν_s(OCO) vibration frequency was calculated at 1293 cm^{-1} with 709 $km \cdot mol^{-1}$ intensity, corresponding to a strong adsorption at 1273 cm^{-1} (Figures 1−3). However, as shown in Figures 1 and 2, the peak intensity at 1273 cm^{-1} increased initially and then decreased with time, while the peak at 1545 cm^{-1} did not decrease at all due to the

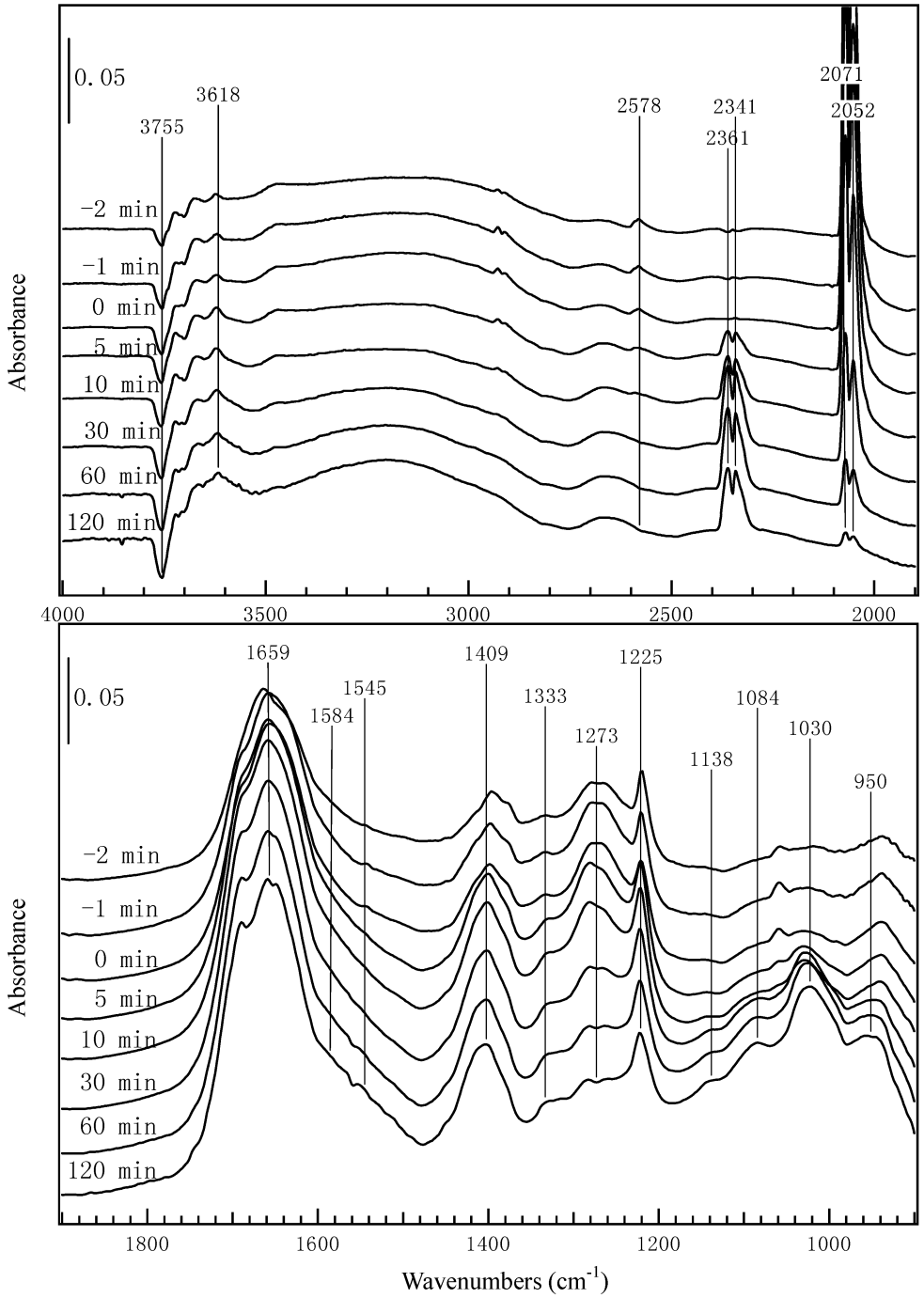

Figure 1. Dynamic changes of in situ DRIFTS spectra in closed system for MgO at 303 K after 1000 ppm OCS balanced with moist air was introduced into the in situ infrared chamber. (Negative time denotes the time before the in situ-DRIFTS chamber was closed.)

effect of the strong band at 1584 cm^{-1} of carbonate.[34] So, the bands of *X* at 1273 cm^{-1} and another band at 1545 cm^{-1} can be assigned to ν_{as}(OCO) and ν_s(OCO) of $HSCO_2^-$ on MgO.

3.3. Heterogeneous Reaction of OCS on MgO in Flow System. In order to analyze the gaseous products and to investigate the effects of oxygen, surface hydroxyl, and water on the heterogeneous reaction, the experiments were performed in a flow system. The dynamic changes of in situ DRIFTS spectra of MgO were measured in the flow system upon sequential introduction of dry OCS/N_2 and dry OCS/air. Gaseous products were simultaneously analyzed by QMS on-line, and the results are presented in Figure 5−7.

Figure 5 shows the mass spectrum of gaseous products of 1000 ppm OCS in dry nitrogen and dry air at 303 K over MgO. There are four main peaks at mass numbers of 34, 44, 60, and 64 in the range of 33−70 amu, which belong to H_2S, CO_2, OCS, and SO_2 respectively. The peak at 44 also includes the CS fragment peak of OCS, and the peak at 48 is the SO fragment peak of SO_2. Therefore, we can conclude that gaseous products of heterogeneous reaction of OCS over MgO include CO_2, H_2S, and SO_2.

Figure 6 shows the dynamic changes of in situ DRIFTS spectra for the MgO sample exposed to a flow of dry 1000 ppm of OCS/N_2 and then dry OCS/air at 303 K. The surface HS, which is formed from the dissociative adsorption of H_2S on MgO,[38,39] was observable in dry nitrogen (Figure 6A, spectra a−d), while it decreased quickly when O_2 was introduced into the feed gas (Figure 6A, spectra e−h). We also observed the decrease of HS at 2578 cm^{-1} in intensity as a function of time in Figures 1 and 2. The band at 1333 cm^{-1} for SO_2[32,33] increased

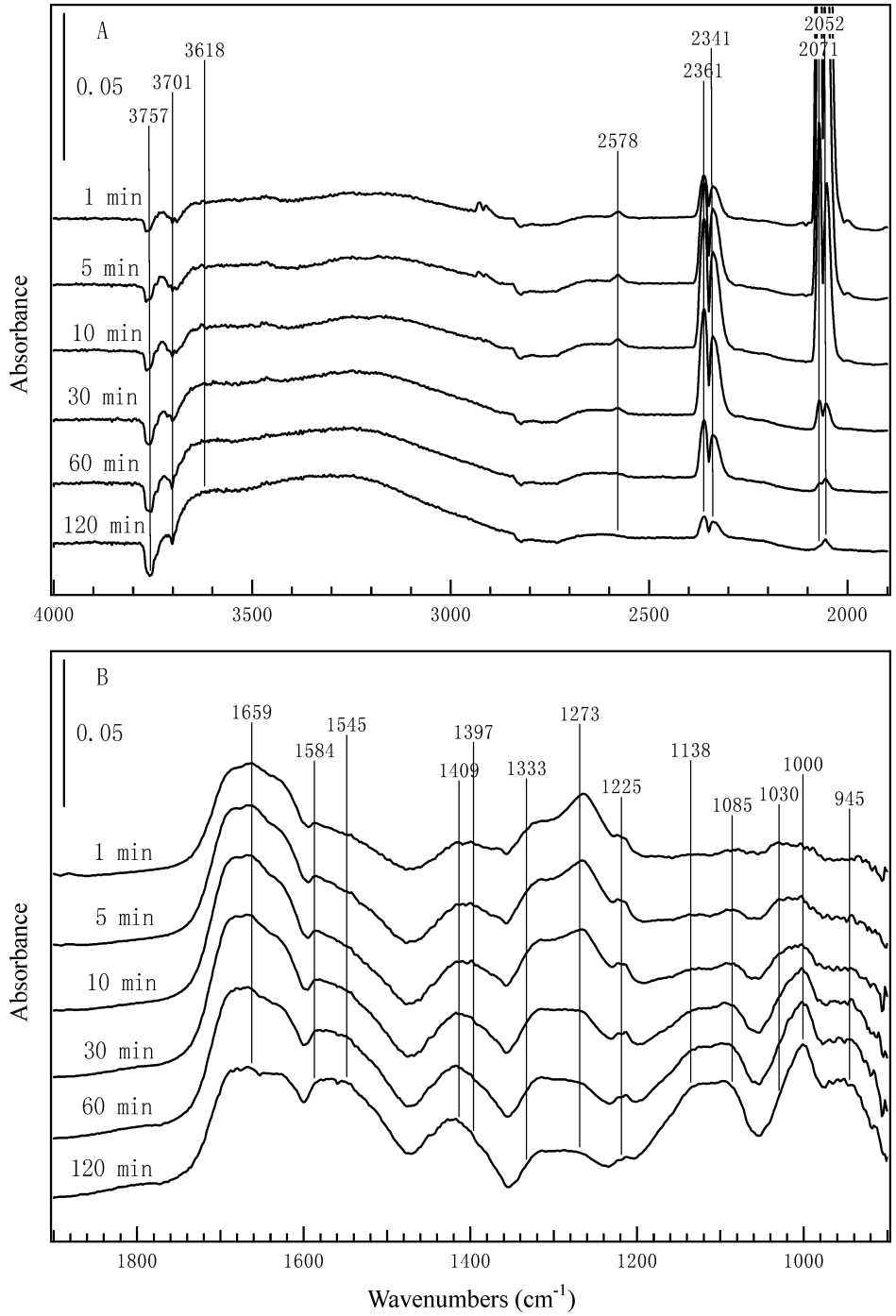

Figure 2. Dynamic changes of in situ DRIFTS spectra in closed system for MgO at 303 K after 1000 ppm OCS balanced with dry air was introduced into the in situ infrared chamber.

initially (Figure 6B) and then decreased when O_2 was introduced into the system, which was accompanied by the increase in intensity of surface sulfate at 1178 and 1138 cm^{-1}[29,31] and surface sulfite in the range of 1084−950 cm^{-1}.[24,35,36] This means gaseous SO_2 is related to the oxidation of H_2S or surface HS by surface oxygen species and then SO_2 is further oxidized to surface sulfite and sulfate by gaseous oxygen or surface oxygen.

Even without water in the feed gas, heterogeneous reaction of OCS on MgO also took place for a moment, which was well supported by DRIFTS spectra (Figures 2 and 6) and mass spectroscopy for gaseous products (Figure 5). Therefore, it can be deduced that surface OH is related not only to the formation of $HSCO_2^-$ but also to the decomposition of $HSCO_2^-$ to produce HCO_3^-, CO_2, and H_2S. Liu et al.[14] also reported surface OH on Al_2O_3 has an important effect on the reaction rate of OCS on Al_2O_3. Figure 7 shows the effect of H_2O on the reaction of OCS over MgO. After reaction with 1000 ppm OCS in moist N_2 for 30 min, the MgO sample was purged with N_2 till the gaseous OCS disappeared thoroughly (Figure 7, spectra a), and then purged with moist simulated air for 180 min (Figure 7, spectra b). The intensity of $HSCO_2^-$ (1273 cm^{-1}) and surface OH (3757 cm^{-1}) decreased remarkably as shown in Figure 7. However, the decrease at 1545 cm^{-1} is not clear due to the effect of the strong band at 1584 cm^{-1} from carbonate.[34] This means that surface OH also participates in the decomposition of $HSCO_2^-$ even in the presence of H_2O in the reaction system. On the other hand, when O_2 was introduced into the feed gas, the intensity in the range of 3300−3500 cm^{-1} increased a little,

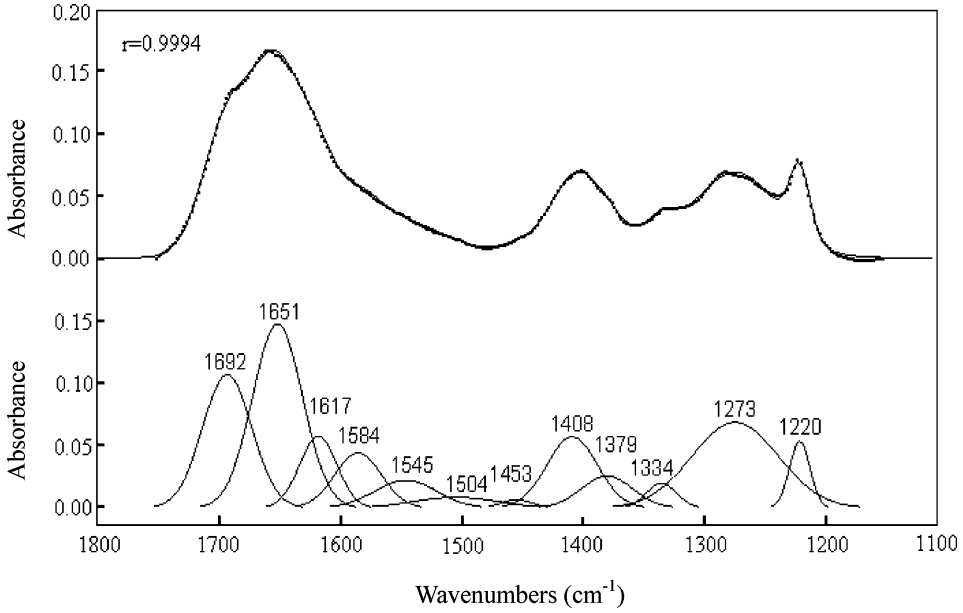

Figure 3. Peak fit of DRIFTS spectrum in the range of 1150−1750 cm^{-1} after reaction for 10 min in Figure 1.

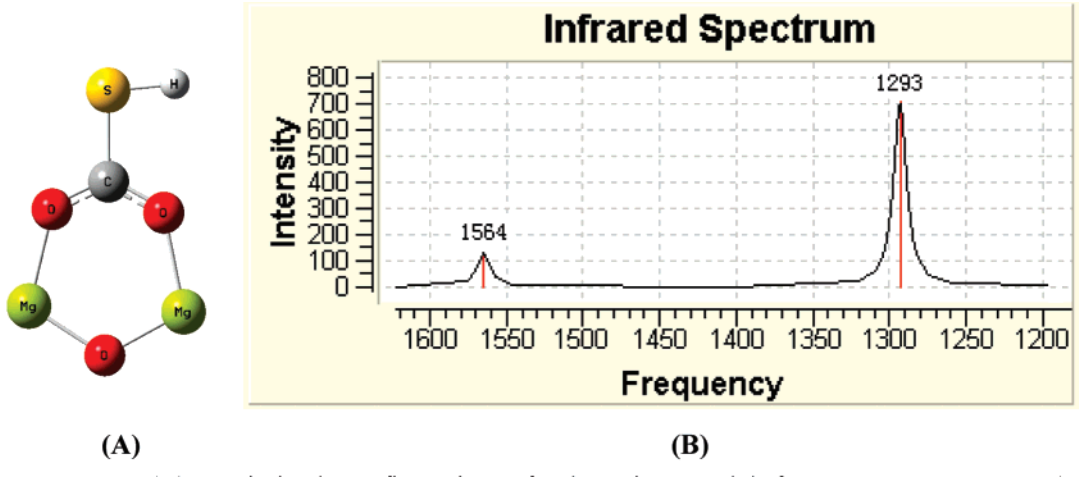

Figure 4. (A) Optimized configuration of adsorption model for $HSCO_2^-$ on MgO and (B) calculated vibrational IR spectrum for $HSCO_2^-$.

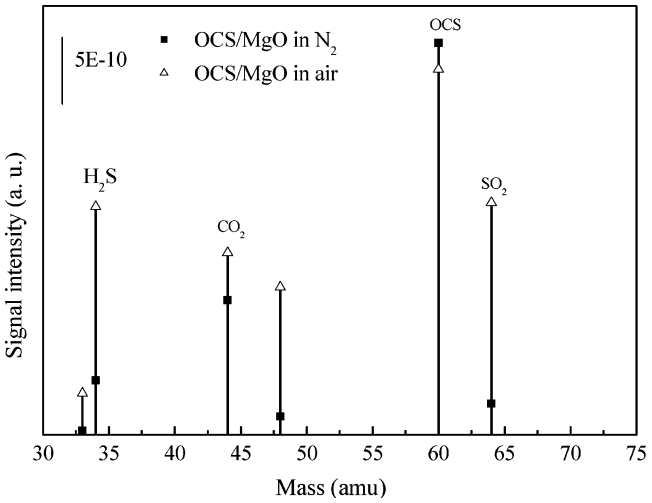

Figure 5. Mass spectra of gaseous products for 1000 ppm OCS on MgO in dry N_2 and in dry air.

as shown in Figure 6, because of the formation of H_2O from H_2S or surface HS oxidized by O_2 or surface O.[40] The newly formed water promotes the hydrolysis of OCS to give rise to more H_2S and CO_2 in turn. Therefore, the QMS signal of gaseous H_2S in the presence of O_2 is much stronger than that in the absence of O_2 in Figure 5. It is well-known that there exists a balance between surface hydroxyl and gaseous water on metal oxides. Accordingly, the lost surface hydroxyl can be compensated partially by gaseous water, which promotes further reaction between surface $HSCO_2^-$ and surface OH in the moist reaction system.

3.4. Mechanism of Heterogeneous Reaction of OCS on MgO. Because the (100) face is the most stable face for MgO (Figure 8A),[38,41,42] the active site, which includes two adjacent surface hydroxyls and one Lewis acid site of magnesium, was put forward as shown in Figure 8B. The possible mechanism of heterogeneous reaction of OCS on MgO could be proposed on the basis of the above results as shown in Figure 9.

First, OCS is adsorbed on the surface of MgO and reacts with surface OH to form surface $HSCO_2^-$ (I). Type I hydrogen thiocarbonate can be transformed to another type of $HSCO_2^-$ (II), accompanied by positive charge transfer from the neighboring Lewis acid site of Mg. Unfortunately, the characteristic frequency of $HSCO_2^-$ (I) was not observed, probably due to the fast transformation from $HSCO_2^-$ (I) to $HSCO_2^-$ (II). In general, the ring structure is favorable in energy; its calculated adsorptive energy is −103.93 kJ·mol^{-1}, while that

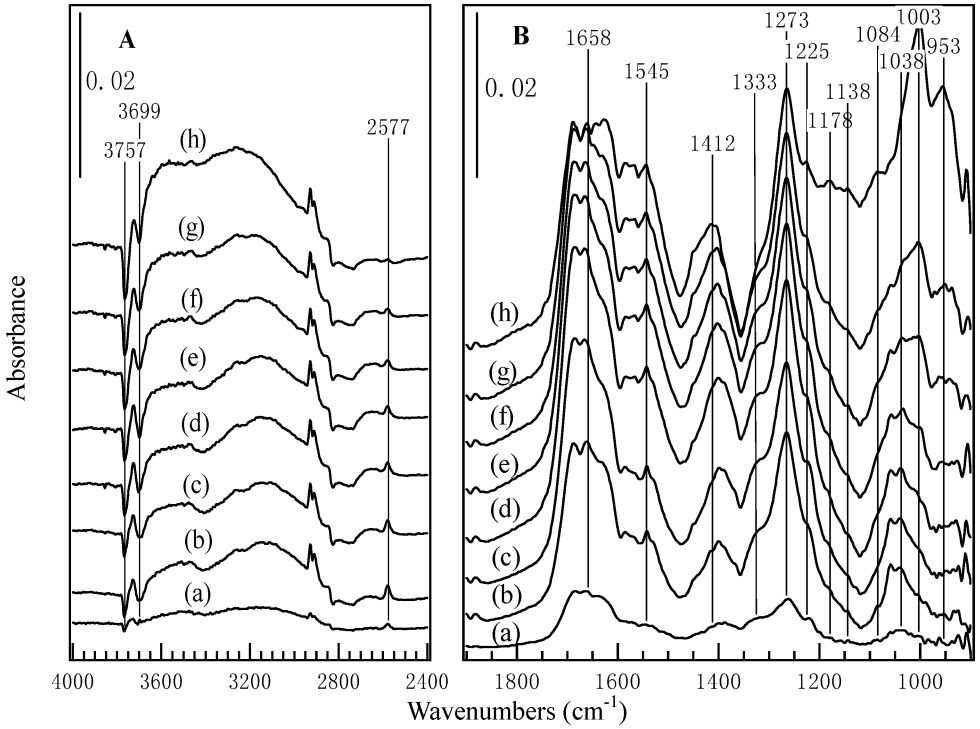

Figure 6. Dynamic changes of in situ DRIFTS spectra for MgO in 1000 ppm OCS in dry N_2 and then in dry air at 303 K in flow system: (a) 1 min in N_2; (b) 5 min in N_2; (c) 10 min in N_2; (d) 30 min in N_2; (e) 1 min in air; (f) 5 min in air; (g) 10 min in air; (h) 30 min in air.

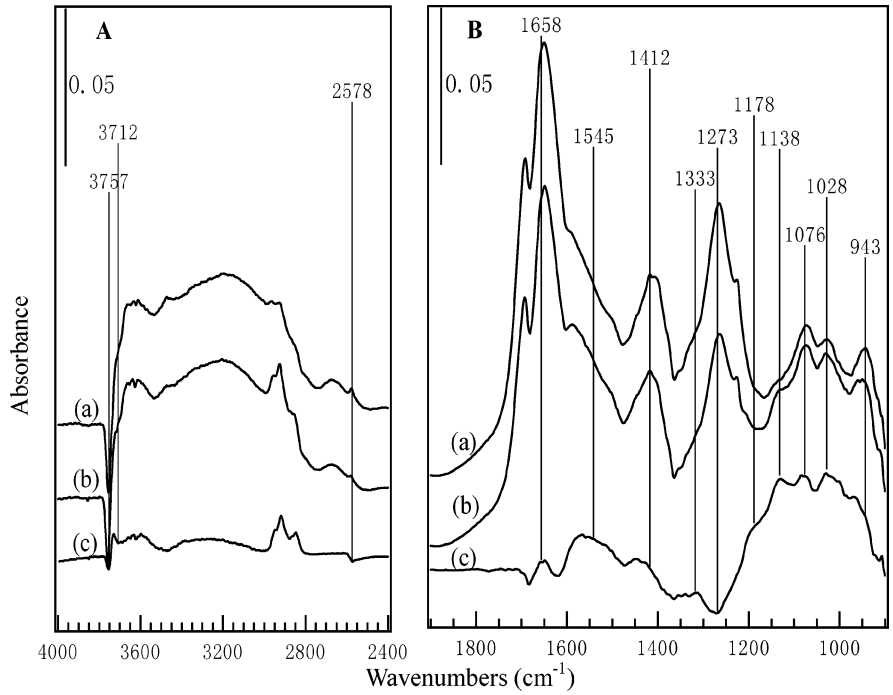

Figure 7. In situ DRIFTS spectra for MgO/OCS in undried flow system at 303 K. (a) MgO reacts with 1000 ppm OCS in N_2 for 30 min and then the system is purged with N_2 utill the gaseous OCS disappears thoroughly. (b) The sample is purged with simulated air for 180 min. (c) The subtracted spectrum of b and a.

for $HSCO_2^-$ (I) is -102.50 kJ·mol^{-1}. Therefore, the main surface species for $HSCO_2^-$ is bridging hydrogen thiocarbonate. The second step of heterogeneous reaction is the decomposition of $HSCO_2^-$ attacked by another adjacent surface OH to produce hydrogen sulfide and bicarbonate. If water is acquirable, the lost surface hydroxyl can be compensated partially by gaseous water, which promotes further reaction between surface $HSCO_2^-$ and surface OH. Finally, H_2S can be dissociatively adsorbed on MgO to generate surface HS and then oxidized to S, SO_2, and HSO_3^-/SO_3^{2-} and SO_4^{2-} by gaseous oxygen or surface oxygen anion radical (O_2^-).[43]

4. Conclusion and Environmental Implication

This study revealed that OCS could be catalytically hydrolyzed by surface hydroxyl on MgO and then the sulfur species can be catalytically oxidized on MgO surface to produce sulfite and sulfate under ambient conditions. Surface hydrogen thiocarbonate was found to be a key intermediate formed by the

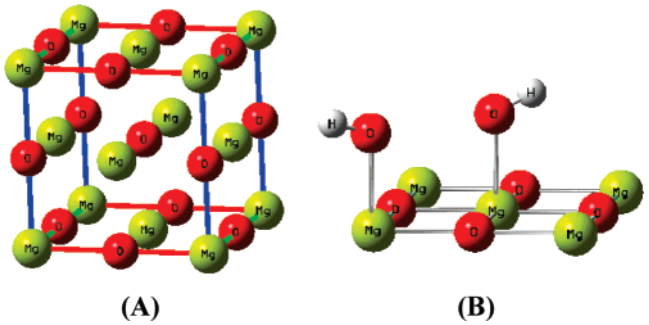

Figure 8. (A) Crystal structure of periclase (MgO) and (B) the structure of active site on MgO (100) face.

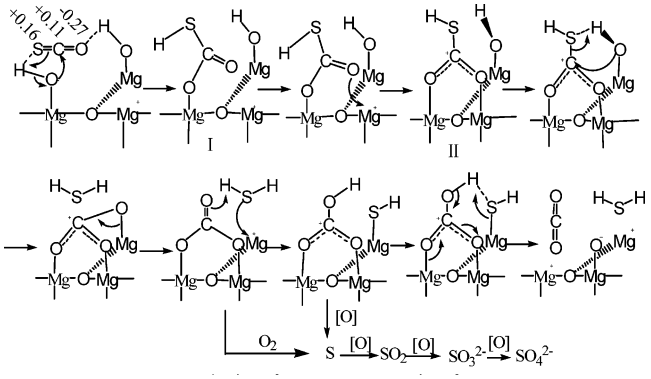

Figure 9. Mechanism of heterogeneous reaction of OCS on MgO.

reaction of OCS with surface hydroxyl. Carbon dioxide, hydrogen sulfide, and sulfur dioxide were also found as the main gaseous products by further reaction between surface hydroxyl and hydrogen thiocarbonate. Surface sulfate is the deep oxidization product of sulfur-containing species through intermediates including sulfide, sulfur, sulfur dioxide, and sulfite in sequence.

Although the content of MgO in mineral atmospheric particles is only 6.1 wt %, which is much lower than that of SiO_2 and Al_2O_3, the basicity of MgO ($pK_a = 9\sim10$) is much stronger than that of SiO_2 ($pK_a \leq 7$) and Al_2O_3 ($pK_a = 7\sim8$),[26,42,44] which is a favorable factor for the hydrolysis of OCS. In addition, because the typical relative humidity in environment is in the range of 20−80%, the active site proposed as above can be easily formed by the adsorption of water on the surface of MgO. Therefore, the reaction of OCS on MgO may be an important path for heterogeneous reaction of OCS on atmospheric particulates. Of course, the similarities and differences among different metal oxides as well as the real mineral particles and the uptake coefficient of OCS on these particles should be studied in detail in future work.

Acknowledgment. This research was financially supported by the National Natural Science Foundation of China (50621804) and 973 Program (2007CB407301).

References and Notes

(1) Turco, R. P.; Whitten, R. C.; Toon, O. B.; Pollack, J. B.; Hamill, P. *Nature* **1980**, *283*, 283−286.
(2) Chin, M.; Davis, D. D. *J. Geophys. Res.* **1995**, *100* (DS), 8993−9005.
(3) Watts, S. F. *Atmos. Environ.* **2000**, *34*, 761−799.
(4) Kjellström, E. J. *Atmos. Chem.* **1998**, *29*, 151−177.
(5) Crutzen, P. J. *Geophys. Res. Lett.* **1976**, *3*, 73−76.
(6) Protoschill-Krebs, G.; Wilhelm, C.; Kesselmeier, J. *Atmos. Environ.* **1996**, *30*, 3151−3156.
(7) Ravishankara, A. R. *Science* **1997**, *276*, 1058−1065.
(8) Andreae, M. O.; Crutzen, P. J. *Science* **1997**, *276*, 1052−1058.
(9) Usher, C. R.; Michel, A. E.; Grassian, V. H. *Chem. Rev.* **2003**, *103*, 4883−4939.
(10) Grassian, V. H. *J. Phys. Chem. A* **2002**, *106*, 806−877.
(11) Ding, J.; Zhu, T. *Chin. Sci. Bull.* **2003**, *48*, 2005−2013.
(12) Corn, M.; Montgomery, T. L.; Reitz, R. J. *Science* **1968**, *159*, 1350−1351.
(13) He, H.; Liu, J. F.; Mu, Y. J.; Yu. Y. B.; Chen, M. X. *Environ. Sci. Technol*. **2005**, *39*, 9637−9642.
(14) Liu, J. F.; Yu, Y. B.; Mu, Y. J.; He, H. *J. Phys. Chem. B* **2006**, *110*, 3225−3230.
(15) West, J.; Williams, B. P.; Young, N.; Rhodes, C.; Hutchings, G. J. *Catal. Commun.* **2001**, *2*, 135−138.
(16) Wu, H. B.; Wang, X.; Cheng, J. M.; Yu, H. K.; Xu, H. X.; Pan, X. X.; Hou, H. Q. *Chin. Sci. Bull.* **2004**, *49*, 739−743.
(17) Zhang, Z. Q.; Friedlander, S. *Environ. Sci. Technol.* **2000**, *34*, 4687−4694.
(18) Frisch, M.; Foresman, J.; Frisch, A.; et al. Gaussian 98. Gaussian Inc.: Pittsburgh, PA, 1998.
(19) Tubergen, M. J.; Lavrich, R. J.; McCargar, J. W. *J. Chem. Educ.* **2000**, *77*, 163−165.
(20) Isoniemi, E.; Petterson, M.; Khriachtchev, L. Lundell, J.; Räsänen, M. *J. Phys. Chem. A* **1999**, *103*, 679−685.
(21) Datta, A.; Cavell, R. G. *J. Phys. Chem.* **1985**, *89*, 450−454.
(22) Peri, J. B.; Hannan, R. B. *J. Phys. Chem.* **1960**, *64*, 1526−1530.
(23) Morterra, C.; Zecchina, A.; Coluccia, S.; Chiorino, A. *J. Chem. Soc., Faraday Trans.* **1977**, *73*, 1544−1560.
(24) Lavalley, J. C. *Catal. Today* **1996**, *27*, 377−401.
(25) Amenomiya, Y.; Morikawa, Y.; Pleizier, G. *J. Catalysis* **1977**, *46*, 431−433.
(26) Rethwisch, D. G.; Dumesic, J. A. *Langmuir* **1986**, *2*, 73−79.
(27) Turek, A. M.; Wachs, I. E.; DeCanio, E. *J. Phys. Chem.* **1992**, *96*, 5000−5007.
(28) O'Grady, A.; Dennis, A. C.; Denvir, D.; McGarvey, J. J.; Bell, S. E. J. *Anal. Chem.* **2001**, *73*, 2058−2065.
(29) Ivanovski, V.; Petruševski, V. M. *J. Mol. Struct.* **2003**, *645*, 273−279.
(30) Bensitel, M.; Waqif, M.; Saur, O.; Lavalley, J. C. *J. Phys. Chem.* **1989**, *93*, 6581−6582.
(31) Wu, Q.; Gao, H. W.; He, H. *J. Phys. Chem. B* **2006**, *110*, 8320−8324.
(32) Datta, A.; Cavell, R. G. *J. Phys. Chem.* **1985**, *89*, 454−457.
(33) Schneider, W. F.; Li, J.; Hass, K. C. *J. Phys. Chem. B* **2001**, *105*, 6972−6979.
(34) Baltrusaitis, J.; Jensen, J. H.; Grassian, V. H. *J. Phys. Chem. B* **2006**, *110*, 12005−12016.
(35) Goodman, A. L.; Li, P.; Usher, C. R.; Grassian, V. H. *J. Phys. Chem. A* **2001**, *105*, 6109−6120.
(36) Miller, F. A.; Wilkings, C. H. *Anal. Chem.* **1952**, *24*, 1253−1294.
(37) Hoggan, P. E.; Aboulayt, A.; Pieplu, A.; Lavalley, J. C. *J. Catal.* **1994**, *149*, 300−306.
(38) Rodriguez, J. A.; Maiti, A. *J. Phys. Chem. B* **2000**, *104*, 3630−3638.
(39) Lavalley, J. C.; Travert, J.; Chevreau, T.; Lamotte, J.; Saur, O. J. C. S. *Chem. Commun.* **1979**, *4*, 146−148.
(40) Liu, C. L.; Chuang, T. T.; Dalla Lana, I. G. *J. Catal.* **1972**, *26*, 474−476.
(41) Valentin, C. D.; Pacchioni, G.; Abbet, S.; Heiz, U. *J. Phys. Chem. B* **2002**, *106*, 7666−7673.
(42) Al-Abadleh, H. A.; Grassian, V. H. *Surf. Sci. Rep*. **2003**, *52*, 63−161.
(43) Sawai, J. *J. Microbiol. Methods* **2003**, *54*, 177−182.
(44) Martin, D.; Duprez, D. *J. Phys. Chem.* **1996**, *100*, 9429−9438.